Electronic Supplementary Material (ESI) for Dalton Transactions.

Electronic Supporting Information

One-pot Synthesis of Oxamidato-Bridged Hexarhenium Trigonal Prisms Adorned with Ester Functionality

R. Nagarajaprakash, R. Govindarajan and Bala. Manimaran*

Department of Chemistry, Pondicherry University, Puducherry, 605014, India

* Corresponding author. Tel.: +91-413-2654 414; fax: +91-413-2656 740

Email: manimaran.che@pondiuni.edu.in

Table S1 Crystallographic Data and Structure Refinement for **4**

Formula	$C_{114}H_{72}N_{12}O_{36}Re_6$
Formula Weight	3303.09
Crystal system	monoclinic
Temperature (K)	150
Space group	*C2/n*
a/Å	34.648(2)
b/Å	27.6088(13)
c/Å	14.0477(9)
α/°	90.00
β/°	101.403(7)
γ/°	90.00
Unit cell volume/Å^3	13172.7(13)
No. of formula units per unit cell, *Z*	4
F(000)	6326.0
D_{calc} (mg mm^{-3})	1.669
Absorption Coefficient (mm^{-1})	5.568
Theta range for data collection (deg)	5.32 to 50.00
Crystal size (mm)	0.4 × 0.4 × 0.1
No. of Reflections measured	28381
No. of Independent reflections	11593
R_{int}	0.0479
Final R_1 values ($I > 2\sigma(I)$)	0.0629
Final $wR(F^2)$ values ($I > 2\sigma(I)$)	0.1562
Final R_1 values (all data)	0.1131
Final $wR(F^2)$ values (all data)	0.1779
Largest diff. peak and hole (e Å^{-3})	2.27 and –2.30
Goodness-of-fit on F^2	1.037
CCDC number	1052630

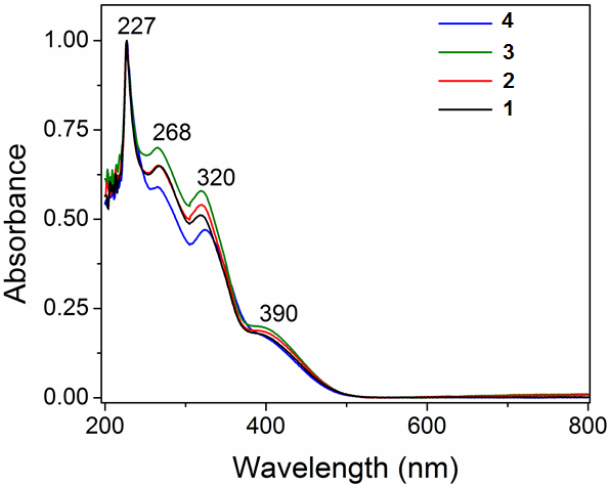

Fig. S1 UV–vis absorption spectra of compounds **1**–**4**.

Experimental Details for UV-vis and Fluorescence titration experiments

3 mL (2×10^{-5} M) stock solution of respective guest in dichloromethane or methanol was prepared and taken in a quartz cell of 1 cm width. 2×10^{-7} M stock solutions of the host **2** were added to the stock solution of guests in an incremental manner and the corresponding absorption spectra were recorded at constant intervals. Fluorescence titration experiments were carried out in an identical fashion.

The binding constants (K_a) were calculated using Benesi-Hildebrand equation (1) from UV–vis spectroscopic titration data.[1]

$$1/\Delta A = 1/\Delta A_{sat} + 1/(\Delta A_{sat}\, K_a\, [host]) \qquad (1)$$

where, ΔA is the change in absorbance of guest upon addition of host and ΔA_{sat} is the maximum absorbance difference. The binding constant (K_a) was evaluated graphically by plotting $1/\Delta A$ versus 1/[host]. The experimentally observed data were linearly fitted according to equation (1) and the K_a values were obtained from the slope and intercept of the line.

The Stern-Volmer constants (K_{SV}) were calculated using Stern-Volmer equation (2) from fluorescence spectroscopic titration data.[2]

$$(I_0/I) = 1 + K_{SV}\, [host] \qquad (2)$$

where, I_0 and I are fluorescence intensities of guest in the absence and presence of host respectively and K_{SV} is Stern-Volmer constant. The experimentally observed data were linearly fitted according to equation (2) and the K_{SV} values were obtained from the slope of the line.

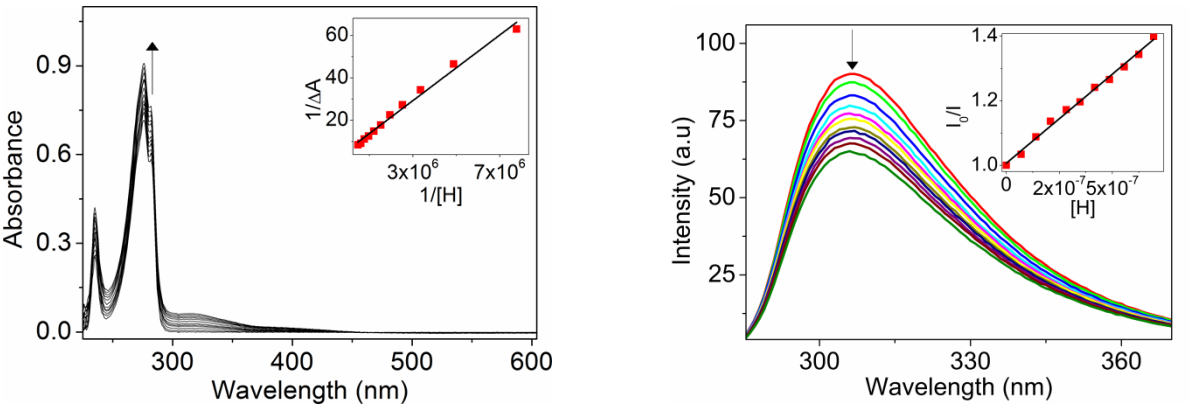

(a) (b)

Fig. S2 (a) Enhancement in absorption pattern of catechol (2.6×10^{-4} M) upon incremental addition of host **2** ($6.7–80 \times 10^{-8}$ M) in dichloromethane and inset shows the corresponding Benesi-Hildebrand plot. Regression analysis was carried out at λ_{max} 282 nm. (b) Emission intensity of catechol (2.6×10^{-4} M) decreasing with incremental addition of host **2** ($6.7–80 \times 10^{-8}$ M) and inset shows the corresponding Stern-Volmer plot. Regression analysis was carried out at λ_{max} 306 nm.

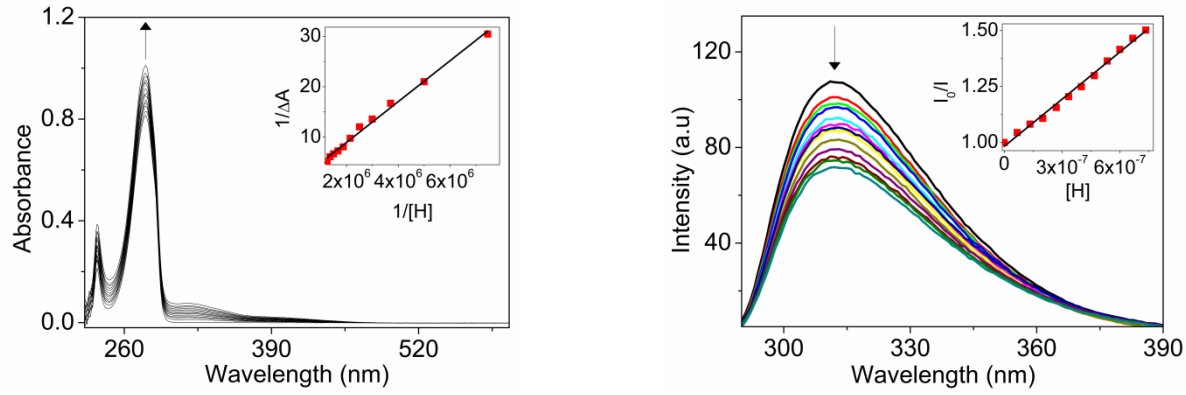

(a) (b)

Fig. S3 (a) Enhancement in absorption pattern of resorcinol (2.6×10^{-4} M) upon incremental addition of host **2** ($6.7–80 \times 10^{-8}$ M) in dichloromethane and inset shows the corresponding Benesi-Hildebrand plot. Regression analysis was carried out at λ_{max} 279 nm. (b) Emission intensity of resorcinol ($2.6 \times$

10^{-4} M) decreasing with incremental addition of host **2** (6.7–80 × 10^{-8} M) and inset shows the corresponding Stern-Volmer plot. Regression analysis was carried out at λ_{max} 311 nm.

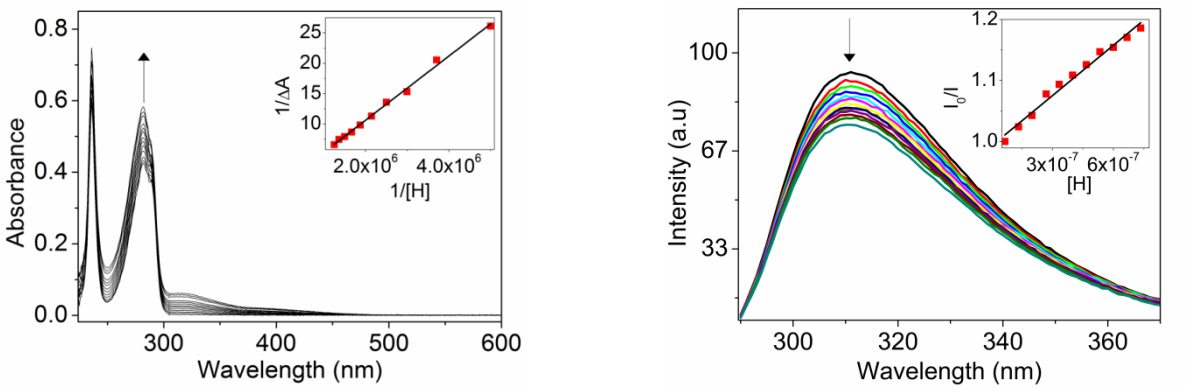

(a) (b)

Fig. S4 (a) Enhancement in absorption pattern of *p*-chloro-*m*-cresol (2.6 × 10^{-4} M) upon incremental addition of host **2** (6.7–80 × 10^{-8} M) in dichloromethane and inset shows the corresponding Benesi-Hildebrand plot. Regression analysis was carried out at λ_{max} 282 nm. (b) Emission intensity of *p*-chloro-*m*-cresol (2.6 × 10^{-4} M) decreasing with incremental addition of host **2** (6.7–80 × 10^{-8} M) and inset shows the corresponding Stern-Volmer plot. Regression analysis was carried out at λ_{max} 311 nm.

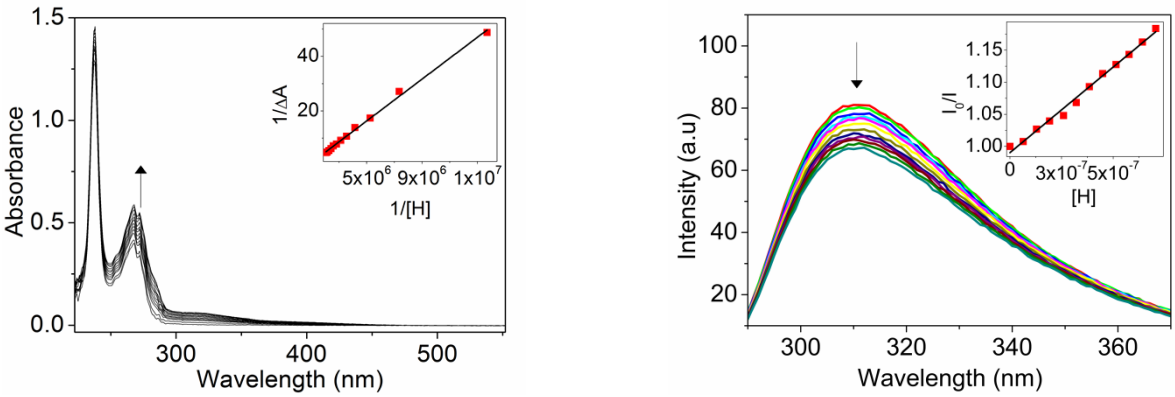

(a) (b)

Fig. S5 (a) Enhancement in absorption pattern of phloroglucinol (1.3 × 10^{-3} M) upon incremental addition of host **2** (6.7–80 × 10^{-8} M) in dichloromethane and inset shows the corresponding Benesi-

Hildebrand plot. Regression analysis was carried out at λ_{max} 273 nm. (b) Emission intensity of phloroglucinol (1.3×10^{-3} M) decreasing with incremental addition of host **2** ($6.7–80 \times 10^{-8}$ M) and inset shows the corresponding Stern-Volmer plot. Regression analysis was carried out at λ_{max} 310 nm.

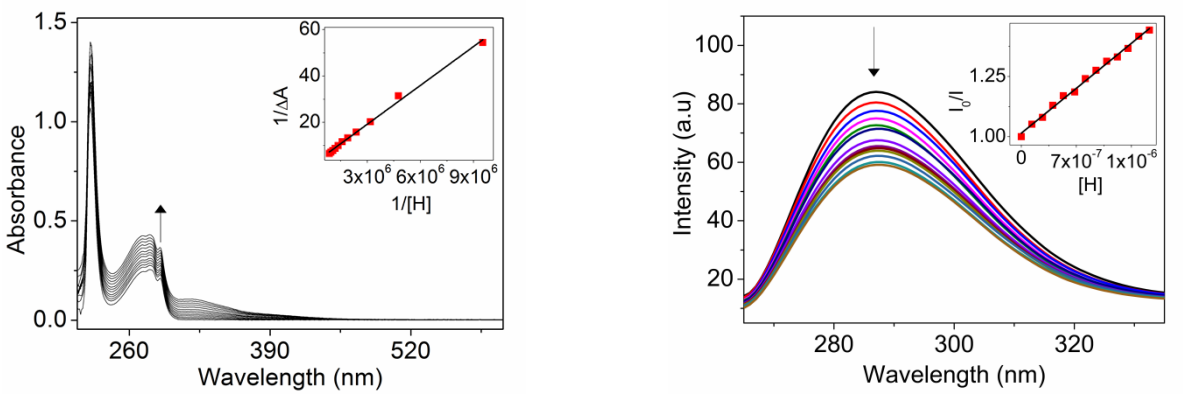

(a) (b)

Fig. S6 (a) Enhancement in absorption pattern of L-tryptophan (1.4×10^{-5} M) upon incremental addition of host **2** ($1.3–16 \times 10^{-7}$ M) in methanol and inset shows the corresponding Benesi-Hildebrand plot. Regression analysis was carried out at λ_{max} 289 nm. (b) Emission intensity of L-tryptophan (1.4×10^{-5} M) decreasing with incremental addition of host **2** ($1.3–16 \times 10^{-7}$ M) and inset shows the corresponding Stern-Volmer plot. Regression analysis was carried out at λ_{max} 287 nm.

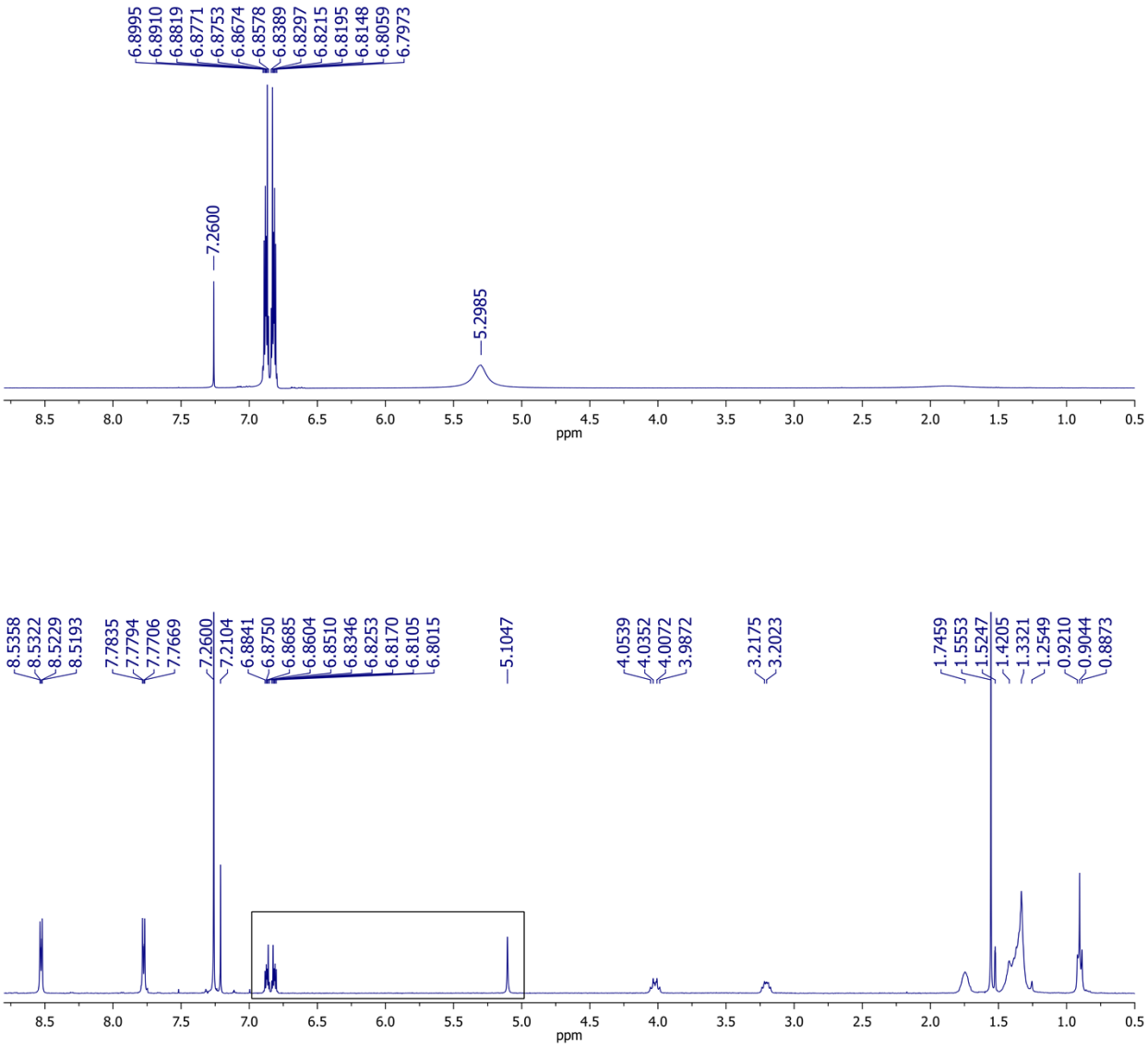

Fig. S7 (Top) ^{1}H NMR spectrum of catechol in $CDCl_3$. (Bottom) ^{1}H NMR spectrum of mixture of **2** and catechol (1:3) in $CDCl_3$, in which the signals corresponding to guest species are shown enclosed in a rectangle.

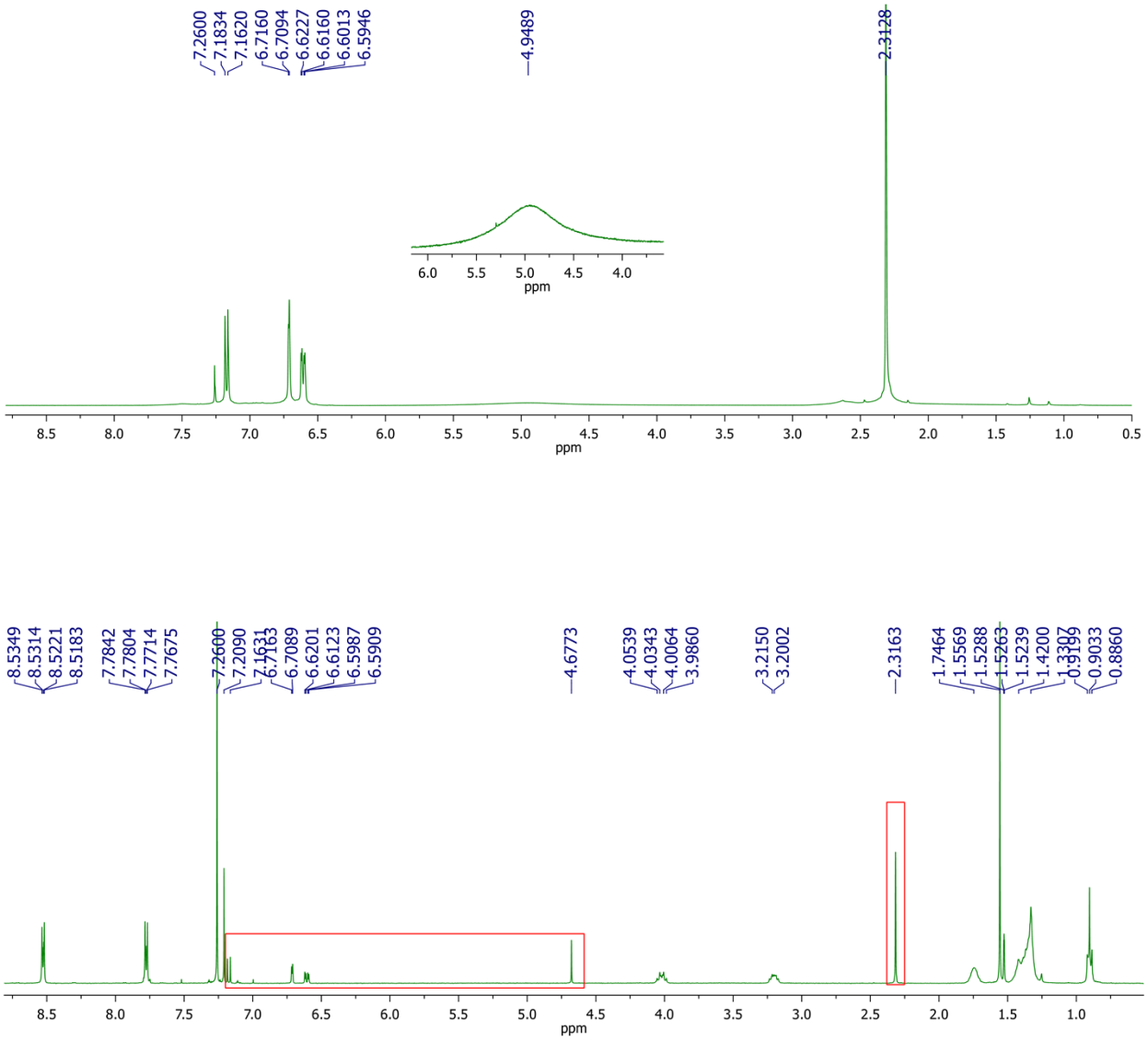

Fig. S8 (Top) ^{1}H NMR spectrum of *p*-chloro-*m*-cresol in $CDCl_3$. (Bottom) ^{1}H NMR spectrum of mixture of **2** and *p*-chloro-*m*-cresol (1:3) in $CDCl_3$, in which the signals corresponding to guest species are shown enclosed in a rectangle.

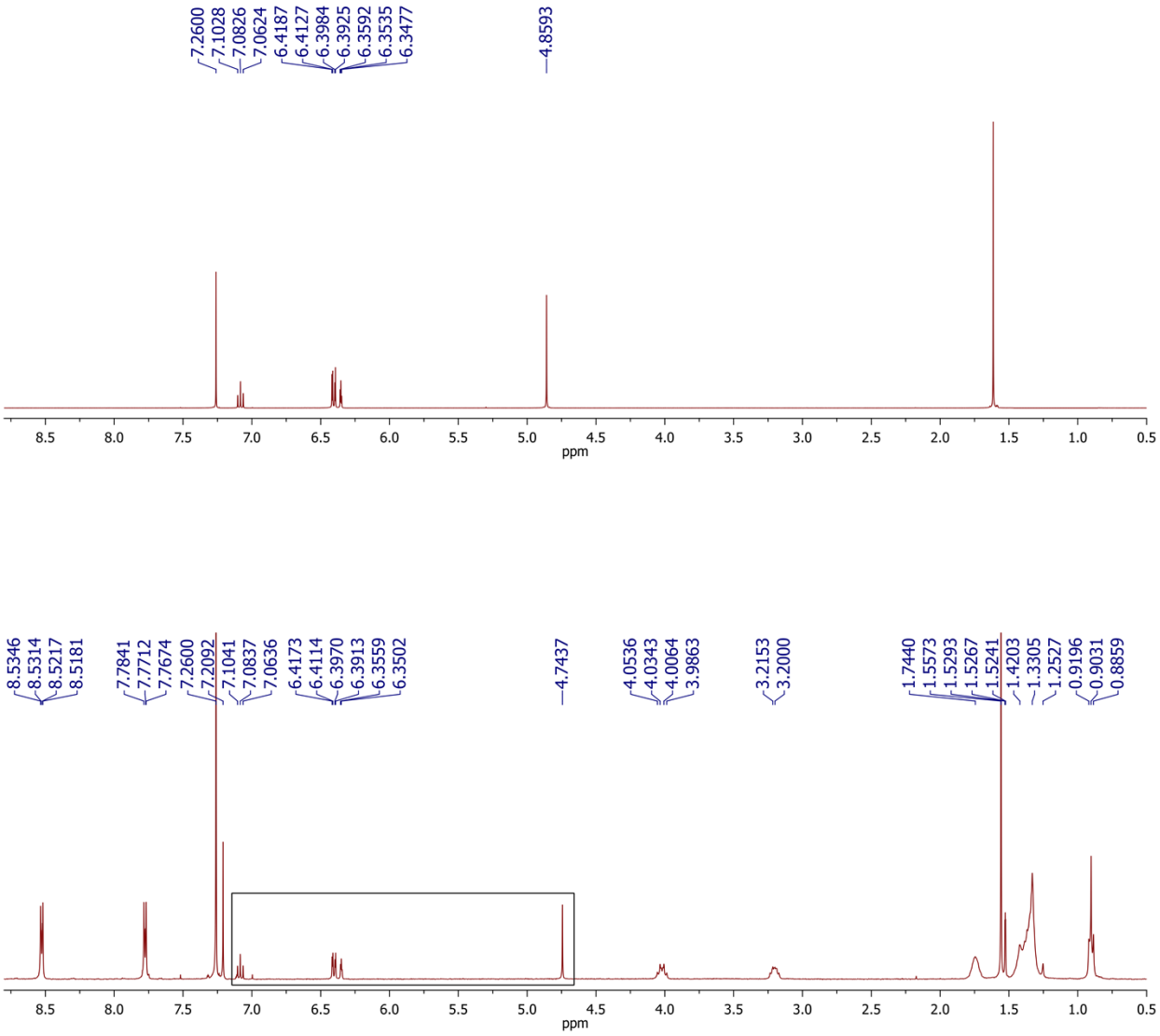

Fig. S9 (Top) ^{1}H NMR spectrum of resorcinol in $CDCl_3$. (Bottom) ^{1}H NMR spectrum of mixture of **2** and resorcinol (1:3) in $CDCl_3$, in which the signals corresponding to guest species are shown enclosed in a rectangle.

Experimental details for Molecular Aggregation studies

Stock solution of **2** and **3** (2×10^{-5} M) in CH_3CN were prepared. 0.5 mL of stock solution was transferred to 5 mL volumetric flask and made up to 5 mL using CH_3CN and H_2O in the following ratio: (i) 100% CH_3CN, (ii) 90% CH_3CN:10% H_2O, (iii) 80% CH_3CN:20% H_2O, (iv) 70% CH_3CN:30% H_2O, (v) 60% CH_3CN:40% H_2O, (vi) 50% CH_3CN:50% H_2O, (vii) 40% CH_3CN:60% H_2O, (viii) 30% CH_3CN:70% H_2O, (ix) 20% CH_3CN:80% H_2O, (x) 10% CH_3CN:90% H_2O. The solutions were allowed to stand for 1 h before recording the emission spectra. The solutions remained homogenous without precipitation even after 24 h. Emission quantum yields, Φ_{em}, were calculated by relative method, based on the comparison of areas of the fluorescence spectra of a reference ($[Ru(bpy)_3]_2^+$, $\Phi_{em} = 0.042$) and of the sample.[3,4] There were no significant changes in the emission pattern up to 50% water content for **2** and **3**.

Table S2 Photophysical data of **2**

Solvent Composition (%)		λ_{max}^{em} **(nm)**	Φ_{em}
CH_3CN	**H_2O**		
100	0	609	1.62×10^{-3}
40	60	602	2.45×10^{-3}
30	70	590	2.84×10^{-3}
20	80	571	7.89×10^{-3}
10	90	566	1.06×10^{-2}

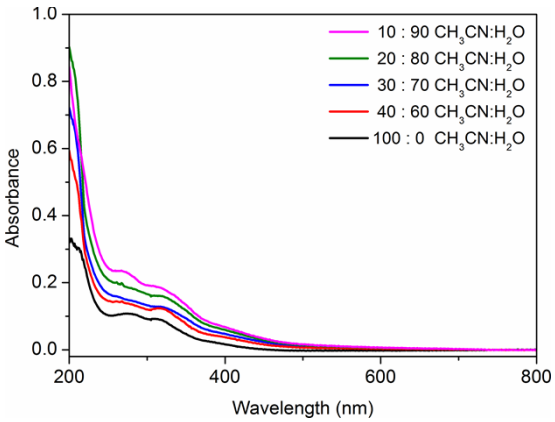

Fig. S10 UV–vis absorption spectra of **2** with increasing H_2O content.

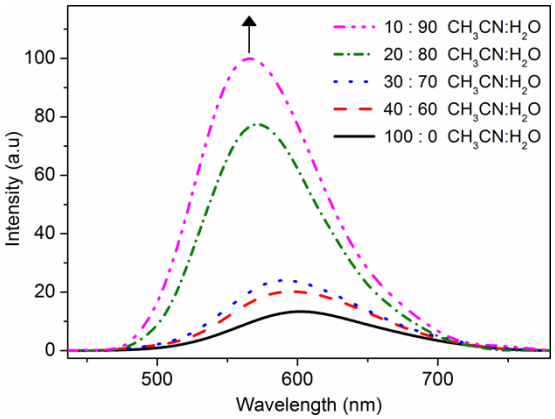

Fig. S11 Normalized overlay emission spectra of **2** in CH_3CN, showing emission enhancement upon increasing H_2O content.

Table S3 Photophysical data of **3**

Solvent Composition (%)		λ_{max}^{em} **(nm)**	Φ_{em}
CH_3CN	**H_2O**		
100	0	611	2.67×10^{-3}
40	60	602	1.61×10^{-3}
30	70	592	2.12×10^{-3}
20	80	566	1.39×10^{-2}
10	90	567	2.05×10^{-2}

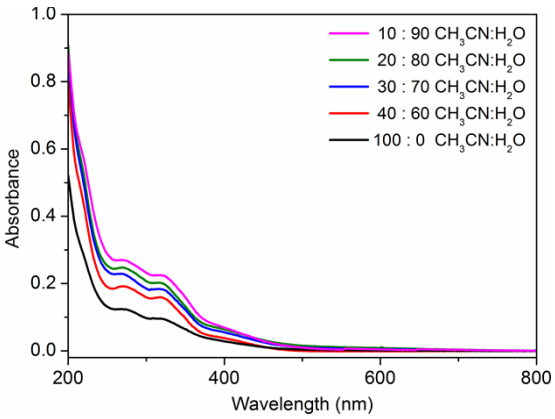

Fig. S12 UV–vis absorption spectra of 3 with increasing H_2O content.

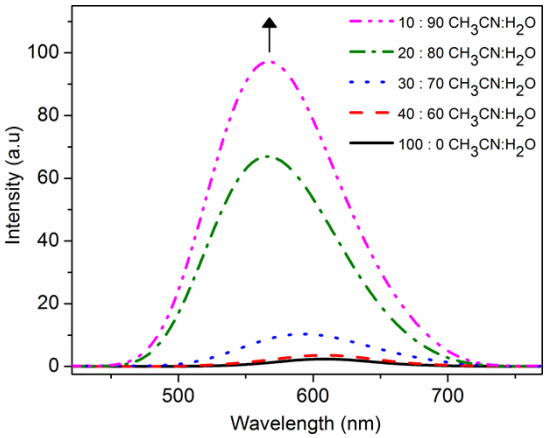

Fig. S13 Normalized overlay emission spectra of **3** in CH_3CN, showing emission enhancement upon increasing H_2O content.

REFERENCES

1. (a) H. A. Benesi and J. H. Hildebrand, *J. Am. Chem. Soc*. 1949, **71**, 2703. (b) S. Shanmugaraju, A. K. Bar and P. S. Mukherjee, *Inorg. Chem.* 2010, **49**, 10235. (c) B. Manimaran, L. J. Lai, P. Thanasekaran, J. Y. Wu, R. T. Liao, T. W. Tseng, Y. H. Liu, G. H. Lee, S. M. Peng and K. L. Lu, *Inorg. Chem*. 2006, **45**, 8070.

2. (a) O. Stern, and M. Volmer, *Phys. Z.* 1919, **20**, 183. (b) S. Shanmugaraju, A. K. Bar, S. A. Joshi, Y. P. Patil and P. S. Mukherjee, *Organometallics* **2011**, *30*, 1951–1960. (c) S.

Shanmugaraju, V. Vajpayee, S. Lee, K. W. Chi, P. J. Stang and P. S. Mukherjee, *Inorg. Chem.* 2012, **51**, 4817.

3. P. Thanasekaran, J. Y. Wu, B. Manimaran, T. Rajendran, I. J. Chang, S. Rajagopal, G. H. Lee, S. M. Peng and K. L. Lu, *J. Phys. Chem. A* 2007, **111**, 10953.

4. D. P. Rillema, G. Allen, T. J. Meyer and D. Conrad, *Inorg. Chem.* 1983, **22**, 1617.